The Thermal Stability of Quenched and Partitioned Steel Microstructures

Koopmans, T.T.W.; Sietsma, Jilt; Zhao, Lie; Santofimia, Maria J.

Important note
To cite this publication, please use the final published version (if applicable).
Please check the document version above.

The Thermal Stability of Quenched and Partitioned Steel Microstructures

Tjerk Koopmans, Jilt Sietsma,* Lie Zhao, and Maria J. Santofimia

Dedicated to Professor Wolfgang Bleck on the occasion of his 70th birthday.

The quenching and partitioning (Q&P) process is a heat treatment process, aiming at the creation of steel microstructures composed of martensite and retained austenite. Herein, the thermal stability of the microstructure is investigated upon reheating steel microstructures, created with different Q&P settings, in different thermal routes, using dilatometry and thermomagnetometry to quantitatively monitor phase fractions. Analysis of the derivative of dilatometry curves and thermomagnetic data reveals that upon reheating the retained austenite decomposes. The decomposition occurs in two stages when the heating rate is relatively low. The retained austenite completely transforms to ferrite and cementite upon reheating to 550 °C, followed by isothermal holding for 1800 s. Increasing the partitioning time from 50 to 300 s at 400 °C after quenching to 260 °C significantly increases the thermal stability of retained austenite. In all conditions, both carbon-depleted martensite (formed in the initial quenching step) and fresh martensite (formed in final Q&P quenching) are found to be partially tempered during the reheating experiments.

1. Introduction

Steels having microstructures mainly composed of martensite and retained austenite form a group of materials in development designed to achieve the excellent combinations of strength and ductility required for the third generation of advanced high-strength steels for the automotive industry.[1–3] Within the concepts currently being studied for the development of these types of microstructures, one of the most intensively investigated subjects is the so-called quenching and partitioning (Q&P) process.[4–27] The Q&P process consists of austenitization followed by fast cooling to a temperature below the martensite start temperature to form a controlled fraction of martensite. This temperature is referred to as quenching temperature (T_Q). Then, the material is subjected to an isothermal treatment at the same or higher temperature (typically between 350 and 450 °C) to promote the partitioning of carbon from martensite to the remaining austenite. This temperature is called partitioning temperature (T_P) and the duration of this isothermal step is referred to as partitioning time (t_P). After this isothermal step, the material is quenched to room temperature, during which sufficiently carbon-enriched austenite is retained, whereas the fraction of the austenite that was not sufficiently enriched with carbon transforms to martensite. This secondary martensite has a higher carbon concentration than the martensite formed at the quenching temperature due to carbon partitioning to austenite during the partitioning step. The secondary, or "fresh," martensite is detrimental for mechanical properties.[20] For this reason, Q&P processing routes should be designed, minimizing the possibility of secondary-martensite formation.

A significant number of studies have been published that show the feasibility of the Q&P process to create the envisioned microstructures.[4–24] Also, numerous studies on the physical or numerical modeling of microstructure development have been published.[25–27] However, there are a limited number of studies on the stability of these microstructures in response to postprocessing routes such as thermomechanical processing or galvanizing treatments. Such heat treatments can lead to the decomposition of retained austenite, as already reported for many other steels.[28–30] In addition, martensite is a metastable phase and can be tempered, for instance, by carbide precipitation upon heating.[31] Any change in the martensite/austenite structure of Q&P steel may deteriorate the mechanical properties. Therefore, the knowledge of the microstructural stability of the nonequilibrium phases of Q&P steels is important for proper control of the mechanical properties of the material after postprocessing or at different service temperatures.

T. Koopmans, J. Sietsma, L. Zhao, M. J. Santofimia
Department of Materials Science and Engineering
Delft University of Technology
Mekelweg 2, 2628 CD Delft, the Netherlands
E-mail: J.Sietsma@tudelft.nl

T. Koopmans, L. Zhao
Department of Production Technology
VDL Weweler BV
Ecofactorij 10, 7325 WC Apeldoorn, the Netherlands

The ORCID identification number(s) for the author(s) of this article can be found under https://doi.org/10.1002/srin.202100290.

**ADVANCED
SCIENCE NEWS**
www.advancedsciencenews.com

**steel
research**
international
www.steel-research.de

This work focuses on the thermal stability of martensite and retained austenite in a range of microstructures in low-carbon steel formed in controlled Q&P processes. The stability is investigated by means of reheating the Q&P steels via different thermal routes. The microstructural processes are experimentally studied, mainly by means of dilatometry and thermomagnetometry.

2. Experimental Section

The material used for the present investigations was an alloy designed for the Q&P process. The chemical composition and corresponding thermodynamic transformation temperatures, calculated by ThermoCalc (TCW version 4, Fe alloys database version 6), are shown in **Table 1**. The steel was produced using a laboratory vacuum induction furnace. After casting, the steel was hot rolled to a final thickness of 4 mm and then air cooled. Cylindrical samples for dilatometry of 3.5 mm in diameter and $L_0 = 10$ mm in length were machined, with the axis parallel to the rolling direction.

Heat treatments were applied using a Bähr 805 DIL A/D dilatometer. Different heat treatments were applied to the steel, as shown in **Figure 1**. These are described as follows.

1) *Heat treatments for the creation of different Q&P microstructures* (Figure 1a): Full austenitization is followed by fast cooling to a quenching temperature between 140 and 340 °C, varied in steps of 20 °C. Subsequently, an isothermal partitioning treatment at 400 °C for 50 s was applied, ending by a quench to room temperature. To study the effect of partitioning time on the stability of retained austenite, for the quenching condition of 260 °C, a partitioning time of 300 s was also applied.

2) *Heat treatments upon reheating the Q&P samples with two different heating rates* (Figure 1b): The Q&P microstructures formed in the treatments of Figure 1a were reheated to 700 °C at 5 °C s^{-1} or to 600 °C at 5 °C min^{-1}, ending by a quench to room temperature.

3) *Heat treatments upon reheating the Q&P samples to different isothermal holding temperatures* (Figure 1c): The Q&P microstructures formed in the treatments of Figure 1a were reheated at 5 °C s^{-1} to 350, 450, and 550 °C, respectively, and isothermally held for 1800 s, ending by a quench to room temperature.

4) *Heat treatments to form a fully martensitic microstructure* (Figure 1d): These heat treatments involved the austenitization conditions used in the creation of Q&P microstructures, immediately followed by a quench to room temperature.

The dilatometry data generated during quenching at 50 °C s^{-1} to room temperature in treatment (d) (Figure 1d) were used to fit the kinetics of the martensite formation according to a modified Koistinen−Marburger equation.[32–34] The Koistinen−Marburger parameters for the present composition are $T_{KM} = 313$ °C and $\alpha = 0.0218$ K^{-1}. The experimentally determined martensite start temperature (M_s) was 331 °C. This information facilitated the calculation of the fraction of
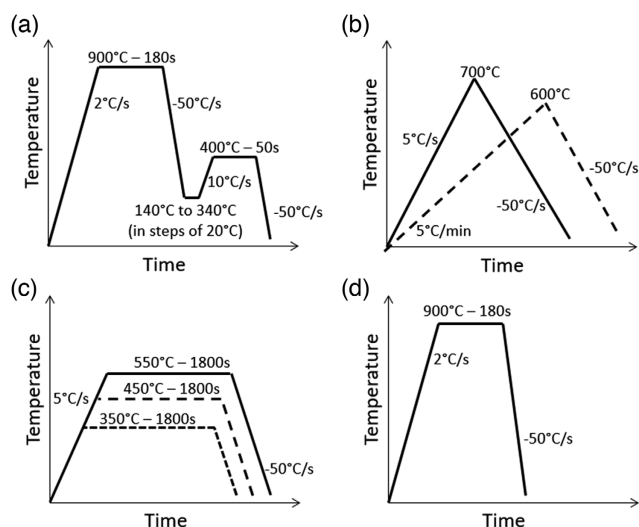

Figure 1. The schematic representation of the applied heat treatments. Note that heat treatments indicated in (b) and (c) were preceded by the heat treatment shown in (a).

martensite formed after quenching to different quenching temperatures.

Dilatometry experiments yielded the length L of the sample, with initial length at room temperature L_0, as a function of time and temperature. The derivative $\frac{d}{dT}\left(\frac{\Delta L}{L_0}\right)$ of the dilatometry data was found to provide a higher resolution than $\Delta L/L_0$ to detect the changes due to the relative expansion and relative contraction caused by phase transformations like decomposition of retained austenite or precipitation of carbides from martensite during heating.[35–37] The derivative curves were calculated from a 20-point simple moving average of both length change and temperature.

After completion of the thermal cycles, two discs with a thickness of ≈2 mm were cut perpendicular to the sample axis and next to each other from one end of the samples. These discs were used for thermomagnetic measurements and X-ray diffraction (XRD) measurements, whereas the resulting surface of the remaining 6 mm-long cylinder was used for microstructural characterization. After the conventional metallographic preparation, samples were etched with 2% nital for optical microscopy and scanning electron microscopy (SEM).[37] SEM observations were conducted with a JEOL JSM-6500 F series field-emission gun SEM, using a secondary-electron imaging detector. The acceleration voltage was 15 kV and the nominal working distance was 10 mm.

Selected samples were metallographically prepared for electron backscatter diffraction (EBSD) examination with a final polishing step of 0.02 μm alumina particles in a neutral solution (OP-AN). EBSD measurements were carried out in a JEOL 6500F series SEM, using an Oxford Instruments Nordlys II detector. The acceleration voltage was 20 kV, the beam current 1.2 nA, the working distance 25 mm, and the tilt angle 70°. 4 × 4 binning of the detector was used. A square grid of 300 × 300 pixels was scanned with a step size of 50 nm, resulting in a scanned area of 15 × 15 μm^2. Acquisition and

Table 1. Chemical composition of the steel in wt%.

C	Mn	Si	Mo	Al	S	P	Fe
0.20	3.51	1.52	0.51	0.03	0.008	0.006	Balance

postprocessing of Kikuchi patterns were conducted using Oxford Instruments Channel 5 software.

XRD experiments were used to determine the volume fraction and the lattice parameter of retained austenite at room temperature. A Bruker D8 Advance Diffractometer equipped with a Vantec position-sensitive detector was used, using Co Kα radiation, an acceleration voltage of 45 kV, and a current of 35 mA, whereas the sample was spun at 30 rpm. The measurements were carried out in the 2θ range 40°−130°, using a step size of 0.035° 2θ, with a counting time of 4 s per step. The volume fraction of retained austenite and the corresponding uncertainty were calculated according to the procedure proposed in other studies.[38–40] The lattice parameters of retained austenite were determined from the peak positions of the {111}, {200}, {220}, and {311} peaks by stripping the Co Kα$_2$ intensity, fitting the peaks with a pseudo-Voigt function and correcting the peak position for sample displacement and goniometer errors,[39] based on LaB$_6$ calibration measurements. Using the lattice parameter, the carbon content in retained austenite was calculated by[35]

$$a = 0.355\,\text{nm} + \left(0.044\,\frac{\text{nm}}{\text{wt\%}}\right)X_c^\gamma \tag{1}$$

where a is the austenite lattice parameter and X_c^γ the weight fraction of carbon in retained austenite. The error in determining the carbon concentration was estimated as 0.05 wt% C.

Magnetic measurements were used to determine the volume fraction of retained austenite at room temperature as well as during reheating of samples with a heating rate from 5 °C min^{-1} to 600 °C. A Lake Shore 7307 vibrating sample magnetometer (VSM) was used to determine the saturation magnetization at room temperature, with a step-wise applied magnetic field up to a field of 2 T. The magnetization as a function of temperature was measured in a constant magnetic field of 1.5 T by reheating the samples in an inserted Lake Shore 73034 oven. The software controlling the VSM was Lake Shore IDEAS-VSM 3.4.0 software. The samples were disc shaped with a diameter of 3.5 mm and a height of ≈2 mm and measured in plane with respect to the magnetic field. The retained austenite volume fraction of each sample, f_γ, was determined from the average saturation magnetization of at least three measurements on the austenite-containing sample, $M_\text{sat}(c)$, by[41]

$$f_\gamma = 1 - \frac{M_\text{sat}(c)}{M_\text{sat}(r)} \tag{2}$$

where $M_\text{sat}(r)$ is the saturation magnetization of a reference austenite-free martensitic sample, confirmed by XRD, to have a volume fraction of austenite less than 1%. The experimental uncertainty in determining the fraction of retained austenite by the magnetic method was less than 1%. An equivalent room-temperature magnetization was calculated according to the methods described in other studies,[42–45] allowing direct calculation of the retained austenite fraction during reheating using Equation (2).

The fractions of retained austenite reported in the present article were determined by a weighted least squares average of the fractions of retained austenite obtained by VSM and XRD. The fractions of martensite formed during the first quench were calculated from a modified Koistinen−Marburger equation and the fractions of bainite were obtained from the dilatometry data during isothermal holding. The fractions of martensite from the second quench were calculated by balancing the volume fractions of the microstructural constituents.

3. Results and Discussion

3.1. Microstructures after Q&P Heat Treatments

The volume fractions of phases present in the steels after different Q&P heat treatments as a function of the quenching temperature are shown in **Figure 2**a and the numerical values are given in **Table 2**. It is found that bainite formation occurs during the partitioning step at quenching temperatures between 240 and 320 °C, with a maximum fraction of 10% at 300 °C. The formation of secondary martensite is fully suppressed when the quenching temperature is lower than 220 °C.
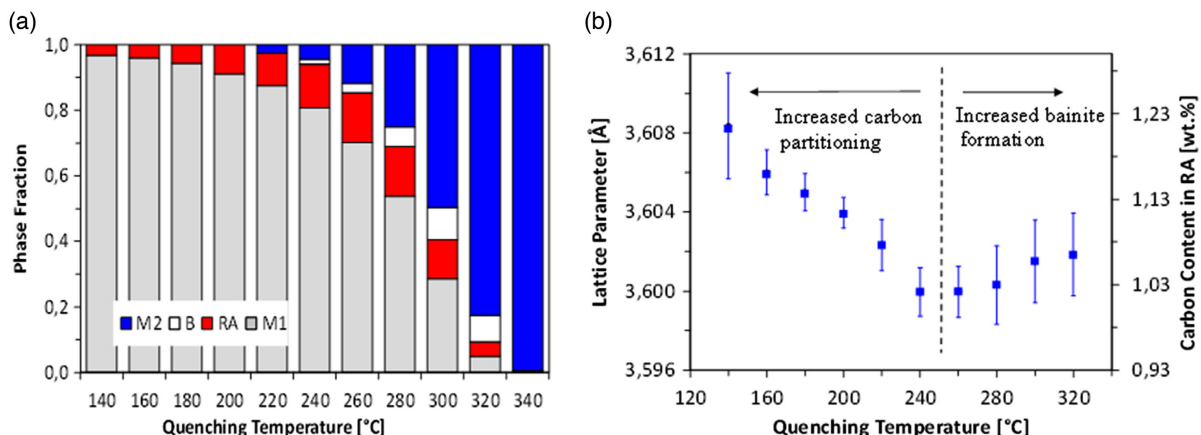

Figure 2. a) Volume fractions of phases present in the samples after Q&P heat treatments shown in Figure 1a. M1: martensite formed in the first quench; B: bainite; RA: retained austenite; and M2: martensite formed in the last quench. b) The lattice parameter of retained austenite and corresponding carbon content.

Table 2. The volume fractions as shown in Figure 2. The uncertainty of the fractions is ≈1% (0.01). The indication "0" indicates a quantity lower than the detection limit of about 1%.

| QT	M1	RA	B	M2
°C				
140	0.967	0.033	0	0
160	0.959	0.041	0	0
180	0.944	0.056	0	0
200	0.911	0.089	0	0
220	0.875	0.099	0	0.025
240	0.807	0.133	0.015	0.045
260	0.702	0.150	0.030	0.118
280	0.538	0.151	0.060	0.251
300	0.286	0.119	0.100	0.496
320	0.050	0.044	0.080	0.826
340	0	0.006	0	0.994

Figure 3. a−c) SEM micrographs and d−e) EBSD phase maps of Q&P samples quenched to a,d) 160 °C, b,e) 260 °C, and c,f) 320 °C. Red in EBSD phase maps represents ferrite, bainite, or martensite; blue represents austenite; and the white pixels are unidentified basically due to low image quality (IQ).

Figure 2b shows the lattice parameter and carbon content of retained austenite as a function of the quenching temperature. When the quenching temperature is lower than 250 °C, the bainite fraction is very low (≈1.5%) and the austenite lattice parameter, representing the carbon concentration in retained austenite, is observed to increase with decreasing quenching temperature. However, the opposite trend is observed in case of significant formation of bainite, as shown in Figure 2b. These results indicate a competition on the source of carbon enrichment of austenite. The main process of carbon enrichment is carbon partitioning from martensite to austenite in the cases in which bainite is not observed and mechanisms associated with the formation of bainite when this phase does form.

The microstructures of the Q&P samples with quenching temperatures of 160, 260, and 320 °C were characterized in detail by means of SEM and EBSD. These samples are selected because they represent three types of microstructures, as shown in Figure 2, and they will be shown in more detail in later sections. Representative microstructures are shown in **Figure 3** and confirm the presence of the phases already shown in Figure 2a. The Q&P sample with quenching temperature 160 °C displays a microstructure consisting of carbon-depleted martensite and retained austenite. The Q&P sample with quenching temperature of 260 °C shows a microstructure containing carbon-depleted martensite as well as carbon-rich martensite formed during the final quenching of the Q&P heat treatment. Films of retained austenite are also observed in this sample. The Q&P sample with quenching temperature 320 °C shows a microstructure formed by carbon-depleted martensite, secondary martensite, bainite, and some retained austenite.

3.2. Reheating to 700 °C at 5 °C s^{-1}

To study the microstructural stability, the Q&P samples were reheated to 700 °C at a heating rate of 5 °C s^{-1} and immediately quenched, as shown in Figure 1b, and then analyzed by XRD and
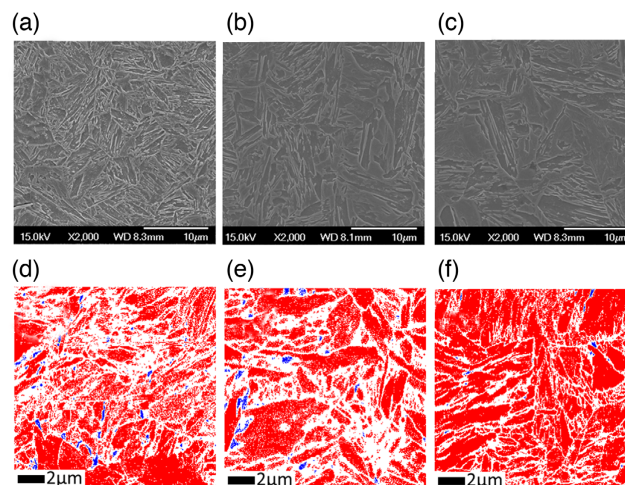
VSM. The volume fraction of retained austenite after this reheating treatment is shown in **Figure 4**a and is compared with the original volume fraction of retained austenite in the Q&P samples. The results show that the volume fraction of retained austenite decreases due to reheating for quenching temperatures between 200 and 300 °C, as shown as region II in Figure 4a. This temperature region corresponds to so-called "the optimum quenching temperature" by which a maximum retained austenite fraction is achieved.[46] At higher and lower quenching temperatures (regions I and III), the observed tendency is the opposite. That is, the volume fractions of retained austenite remain constant or even slightly increase after reheating to 700 °C followed by immediate quenching. Note that the three microstructures of Figure 3 relate to these three temperature regions.

Figure 4b shows the carbon content in retained austenite in Q&P samples before and after reheating to 700 °C at 5 °C s^{-1} followed by quenching to room temperature. The carbon content of the retained austenite remains almost invariable after the reheating of Q&P samples treated at quenching temperatures around the optimum value (region II). Outside that quenching temperature range, the carbon concentration tends to decrease in region I and increase in region III. The results in Figure 4 imply a varying response of retained austenite upon reheating, by promoting more retained austenite in some cases, whereas in other cases, reheating causes austenite decomposition. These observations are further studied in the following sections.

Three distinct quenching temperature regions are shown in Figure 4 with different behaviors of the carbon content and volume fraction of retained austenite as well as different microstructures prior to reheating. The samples were obtained with quenching temperatures of 160 °C (region I), 260 °C (region II), and 320 °C (region III). To study the thermal stability of microstructure upon reheating, the derivative of the length signal from dilatometry is shown in **Figure 5**a, including a reference
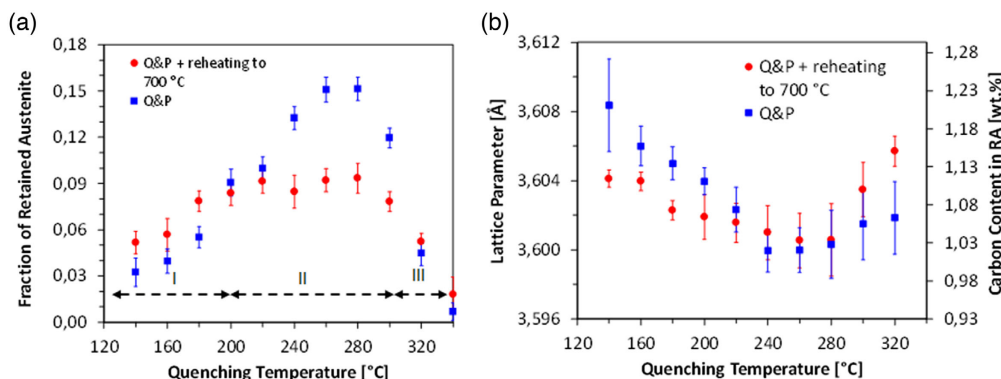
**ADVANCED
SCIENCE NEWS**

www.advancedsciencenews.com

**steel
research**
international

www.steel-research.de

Figure 4. a) Volume fraction of retained austenite in Q&P samples before (blue squares) and after (red circles) reheating to 700 °C at 5 °C s^{-1} followed by quenching. b) The lattice parameter of retained austenite and corresponding carbon content.
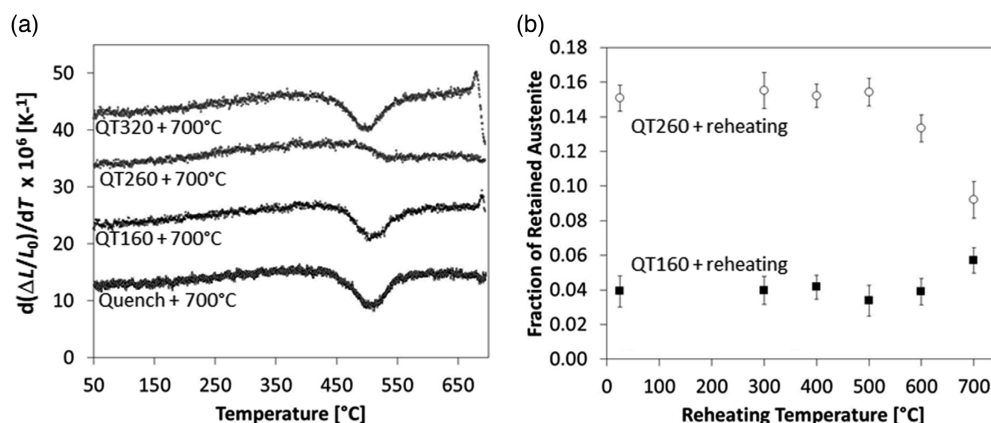

Figure 5. a) Derivative curve calculated from the length change as a function of temperature during heating to 700 °C at 5 °C s^{-1} of Q&P samples with quenching temperatures of 160, 260, and 320 °C and the martensitic microstructure, initially heat treated according to Figure 1d. The curves are shifted to separate them. b) Volume fraction of retained austenite in Q&P samples quenched to 160 and 260 °C after reheating to different temperatures at 5 °C s^{-1} interrupted by quenching.

curve from the sample that fully transformed to martensite, during the heat treatment of Figure 1d. As this microstructure is fully martensitic, the dilatometry curve of this sample only displays the effects of tempering of martensite. The more or less constant value in the plot of Figure 5a indicates the more or less constant coefficient of thermal expansion during heating. A decreasing value indicates the onset of a contraction. Figure 5b shows the austenite fraction of the samples with quenching temperatures of 160 and 260 °C after reheating at 5 °C s^{-1} to various temperatures, up to 700 °C, followed by immediate quenching.

Reheating to 700 °C at 5 °C s^{-1} of the sample with quenching temperature of 160 °C. There is an obvious valley between 450 and 550 °C in the derivative curve in Figure 5a for the samples with quenching temperature of 160 °C, similar to the curve for martensitic sample. Figure 5b shows that there is no significant change in the fraction of retained austenite during heating up to 600 °C. Combining these observations suggests that the valley results from the tempering of martensite via carbide precipitation, possibly including intermediate carbides.[28]

Reheating to 700 °C at 5 °C s^{-1} of the Q&P sample with quenching temperature of 260 °C. The derivative curve for this sample in Figure 5a shows small changes in slope at around 500 °C, probably indicating an overlap between the relative expansion due to the decomposition of retained austenite and a relative contraction due to precipitation of carbides from the martensite. The fraction of retained austenite from the interrupted reheating treatments in Figure 5b shows that the retained austenite starts decomposing at temperatures around 500 °C. The retained austenite fraction in microstructures formed in region II (Figure 4a), to which this sample belongs, is relatively high, and therefore the retained austenite has a relatively low carbon content, giving rise to decomposition upon reheating.

Reheating to 700 °C at 5 °C s^{-1} of the Q&P sample with quenching temperature of 320 °C. This sample also shows a valley between 450 and 550 °C in Figure 5a, similar to the martensitic sample. This valley is again probably associated with precipitation of carbides from martensite, which is the dominant phase in both samples. At ≈680 °C, a change in slope is associated with the

formation of austenite above the Ac1 temperature, taking heating rate into account.[47] The sample with the quenching temperature of 160 °C shows a very small version of this peak, whereas it is not observed for the sample with quenching temperature of 260 °C. It is possible that for the latter sample this small peak would be shifted to a temperature above 700 °C due to a slightly different evolution of austenite decomposition and carbide formation during heating.

3.3. Reheating to 600 °C at 5 °C min^{-1}

As discussed earlier, the decomposition of retained austenite and carbide precipitation from martensite may occur simultaneously in some samples. This overlap could be separated if a relatively slow reheating is applied. Therefore, a dilatometry test was conducted by reheating the three samples that were made by the Q&P treatment of Figure 1a with quenching temperatures of 160, 260, and 320 to 600 °C at a much lower heating rate of 5 °C min^{-1}. **Figure 6**a shows the derivative curves obtained from dilatometry data during this reheating treatment. Analysis of curves leads to the following observations.

Reheating to 600 °C at 5 °C min^{-1} of Q&P samples with quenching temperature of 160 or 320 °C. The derivative curves from the samples quenched to either temperature are similar and are also similar to the ones observed during reheating of the same Q&P samples at 5 °C s^{-1}. In comparison with the ones reheated at a high rate, the valley starts and ends at lower temperatures (around 400 and 500 °C), which is a direct effect of the lower heating rate. Both samples contain a small fraction of retained austenite (around 3%) and thus the decomposition of retained austenite is not observed. The similarity between both curves also implies that the thermal stability of martensite is not significantly influenced by carbon depletion during the partitioning process of the Q&P sample with quenching temperature of 160 °C. This is consistent with the results from numerical simulations,[27] showing that only carbon within a thin shell around the martensite grains is depleted to austenite.

Reheating to 600 °C at 5 °C min^{-1} of the Q&P sample with quenching temperature of 260 °C. Contrary to the derivative curve

for the high heating rate in Figure 5a, the derivative curve in Figure 6a shows two extremes: a (positive) peak between ≈250 and 370 °C and a (negative) valley between 450 and 550 °C. Combined with the results of austenite fraction from in situ thermomagnetic measurements in Figure 6b, it can be understood that the peak results from the decomposition of retained austenite and the valley from the carbide precipitation from martensite, as in this temperature region the austenite fraction is constant. When the temperature increases above to 550 °C, austenite decomposition recommences. This means that decomposition of the retained austenite in this sample during reheating occurs in two stages. This is related to the fact that the retained austenite has different morphology and is formed by different retention mechanisms, also already reported in other steels.[28–30]

3.4. Reheating to and Isothermal Holding at 350, 450, and 550 °C

The microstructure stability upon slow reheating of the Q&P sample with quenching temperature of 260 °C shows the decomposition of retained austenite in two stages (Figure 6). This finding is further investigated by reheating the Q&P samples with quenching temperature of 260 to 350 °C, 450 °C, and 550 °C at 5 °C s^{-1}, followed by isothermal holding at these temperatures for 1800 s and subsequently quenching to room temperature (Figure 1c).

Figure 7 shows the dilatometry curve corresponding to the final quench after isothermal holding the final volume fraction of retained austenite. The three volume fractions of retained austenite after final quenching are 0.135 (350 °C), 0.150 (450 °C), and 0.025 (550 °C). The formation of fresh martensite is not observed after the isothermal treatments at 350 and 450 °C, but it is clearly displayed after isothermal holding at 550 °C, indicating the formation of about 10% martensite with a martensite start temperature of 125 °C. This formation is due to a significant relief of the stress around the remaining austenite as a result of the tempering of martensite at 550 °C. Thus, the remaining
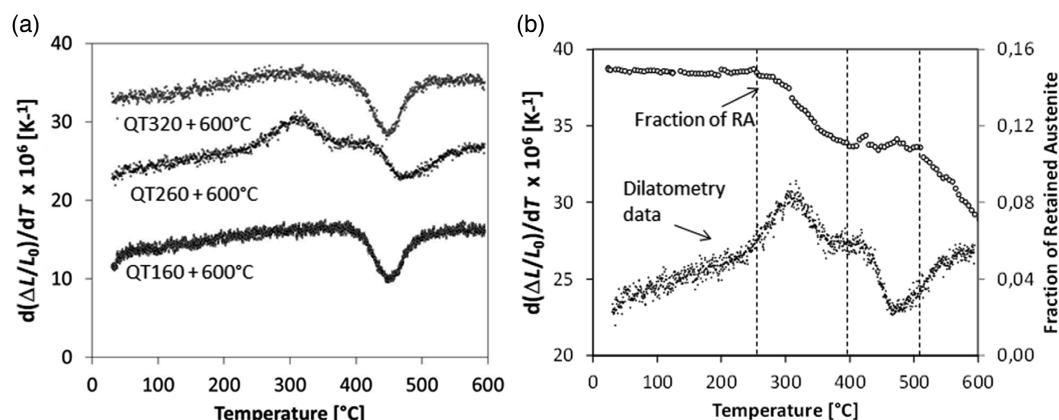

Figure 6. a) Derivative of dilatometry curves during reheating at 5 °C min^{-1} of the Q&P samples quenched to 160, 260, and 320 °C, respectively. b) Comparison of volume fraction of retained austenite determined by the thermomagnetic measurements with the derivative curve for the Q&P sample quenched to 260 °C.
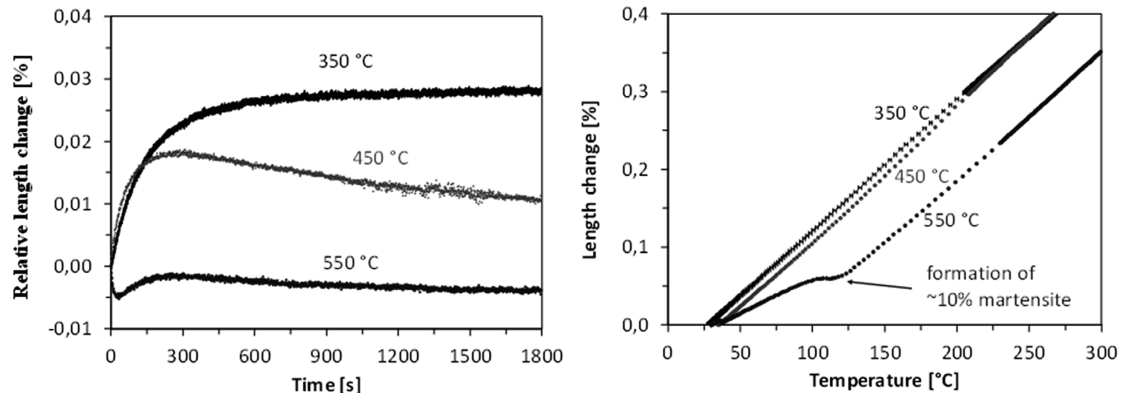
**ADVANCED
SCIENCE NEWS**

www.advancedsciencenews.com

**steel
research**
international

www.steel-research.de

Figure 7. Length change during final quench after isothermal holding at 350, 450, and 550 °C for 1800 s in Q&P samples quenched to 260 °C and reheated to the isothermal holding temperatures at 5 °C s⁻¹.

austenite is destabilized and transforms upon quenching.[11] This stress relief does not occur to a sufficient degree in case of isothermal holding at 350 °C or 450 °C as the temperature is not high enough for carbide precipitation, as shown in Figure 5a. The final fraction of retained austenite in these two samples is slightly lower than that after the Q&P treatment, indicating that only a limited decomposition of retained austenite upon fast heating and subsequent isothermal holding has taken place. The final fraction of retained austenite after isothermal holding at 550 °C is low (2.5%), confirming martensite formation upon quenching.

3.5. The Effect of Longer Partitioning Time

In previous sections, an interesting observation is that the retained austenite in the Q&P samples with quenching temperature 260 °C decomposes in two stages upon slow reheating. In these Q&P samples, the quenching step was followed by partitioning at 400 °C for 50 s. To further study this, the partitioning time was prolonged from 50 to 300 s. **Figure 8** shows the austenite fraction, measured in situ in the magnetometer, during
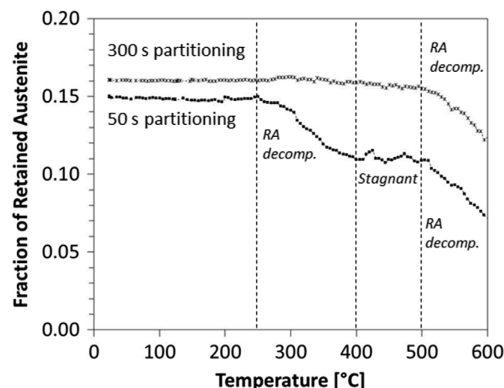

Figure 8. Volume fraction of austenite during reheating to 600 °C at 5 °C min⁻¹, for the Q&P samples quenched to 260 °C and partitioned for 50 and 300 s, respectively.

reheating to 600 °C at 5 °C min⁻¹ for both samples with the partitioning time of 50 and 300 s, respectively. It is found that the austenite present in the sample partitioned for 300 s has a higher thermal stability. The decomposition of retained austenite occurs only at temperatures above 500 °C. A probable reason for the increase in the thermal stability of the austenite is due to the presence of a more homogeneous carbon distribution within the austenite grains, as a result of the longer partitioning time.[27]

4. Conclusion

The thermal stability of microstructures obtained after various Q&P heat treatments in a low-carbon steel is studied upon reheating the samples in the dilatometer and in the magnetometer. The main conclusions are as follows. 1) Upon reheating the Q&P samples quenched to the "optimum" quenching temperature range, the volume fraction of retained austenite decreases, as a result of the partial decomposition and destabilization of retained austenite. When a low reheating rate of 5 °C min⁻¹ is applied, the decomposition initiates at lower temperatures and takes place in two stages, whereas at a high reheating rate of 5 °C s⁻¹, the decomposition overlaps with carbide precipitation. 2) Reheating the Q&P samples to high temperature, for example, to 550 °C for the sample with quenching temperature 260 °C, and isothermal holding for 1800 s leads to almost complete decomposition of retained austenite, in which part of the retained austenite decomposes during heat treatment and part transforms to martensite during subsequent quenching because of destabilization at elevated temperature. 3) When a longer partitioning time is applied, the decomposition of austenite at the lowest temperatures is suppressed, due to a more homogeneous carbon distribution within austenite grains in the Q&P microstructures. 4) Upon reheating, all Q&P samples show partial tempering of martensite. For the Q&P samples quenched outside the "optimum" quenching range, carbide precipitation due to the tempering of martensite is a dominant phenomenon, as the retained austenite itself is stable and the fraction of retained austenite is small.

2100290 (7 of 8)

Conflict of Interest

The authors declare no conflict of interest.

Data Availability Statement

The data that support the findings of this study are available from the corresponding author upon reasonable request.

[1] D. Matlock, J. G. Speer, in *Microstructure and Texture in Steels* (Eds.: A. Haldar, S. Suwas, D. Bhattacharjee), Springer, London **2009**.

[2] J. Zhao, Z. Jiang, *Prog. Mater. Sci.* **2018**, *94*, 174.

[3] B. B. He, B. Hu, H. W. Yen, G. J. Cheng, Z. W. Wang, H. W. Luo, M. X. Huang, *Science* **2017**, *357*, 1029.

[4] J. G. Speer, A. M. Streicher, D. K. Matlock, F. C. Rizzo, G. Krauss, in *Austenite Formation and Decomposition* (Eds: E. B. Damm, M. Merwin), TMS/ISS, Warrendale, PA **2003**.

[5] D. V. Edmonds, K. He, F. C. Rizzo, B. C. De Cooman, D. K. Matlock, J. G. Speer, *Mater. Sci. Eng. A* **2006**, *438–440*, 25.

[6] J. G. Speer, F. C. Rizzo, D. K. Matlock, D. V. Edmonds, *Mater Res.* **2005**, *8*, 417.

[7] M. J. Santofimia, L. Zhao, R. Petrov, J. Sietsma, *Mater. Charact.* **2008**, *59*, 1758.

[8] F. HajyAkbary, J. Sietsma, G. Miyamoto, T. Furuhara, M. J. Santofimia, *Acta Mater.* **2016**, *104*, 72.

[9] E. J. Seo, L. Cho, B. C. De Cooman, *Acta Mater.* **2016**, *107*, 354.

[10] J. Yang, Y. Song, Y. Lu, J. Gu, Z. Guo, *Mater. Sci. Eng. A* **2018**, *712*, 630.

[11] K. O. Findley, J. Hidalgo, R. M. Huizenga, M. J. Santofimia, *Mater. Des.* **2017**, *117*, 248.

[12] J. Hidalgo, K. O. Findley, M. J. Santofimia, *Mater. Sci. Eng. A* **2017**, *690*, 337.

[13] E. De Moor, S. Lacroix, A. J. Clarke, J. Peening, J. G. Speer, *Metall. Mater. Trans. A* **2008**, *39*, 2586.

[14] Z. Dai, R. Ding, Z. Yang, C. Zhang, H. Chen, *Acta Mater.* **2018**, *144*, 666.

[15] P. Huygehe, L. Malet, M. Caruso, C. Georges, S. Godat, *Mater. Sci. Eng. A* **2017**, *701*, 254.

[16] A. Zinsaz-Borujerdi, A. Zarei-Hanzaki, H. R. Abedi, M. Karam-Abian, H. Ding. D. Han, N. Kheradmand, *Mater. Sci. Eng. A* **2018**, *725*, 341.

[17] X. D. Tan, Y. B. Xu, X. L. Yang, Z. P. Hu, F. Peng, X. W. Ju, D. Wu, *Mater. Charact.* **2015**, *104*, 23.

[18] L. B. Luo, W. Li, Y. Gong, L. Wang, X. J. Jin, *J. Iron Steel Res. Inter.* **2017**, *24*, 1104.

[19] E. Paravicini Bagliani, M. J. Santofimia, L. Zhao, J. Sietsma, E. Anelli, *Mater. Sci. Eng. A* **2013**, *559*, 486.

[20] D. De Knijf, R. Petrov, C. Föjer, L. A. I. Kestens, *Mater. Sci. Eng. A* **2014**, *615*, 107.

[21] D. V. Edmonds, J. G. Speer, *Mater. Sci. Tech.* **2010**, *26*, 386.

[22] H. Liu, X. Jin, H. Dong, J. Shi, *Mater. Charact.* **2011**, *62*, 223.

[23] M. J. Santofimia, L. Zhao, R. Petrov, C. Kwakernaak, W. G. Sloof, *Acta Mater.* **2011**, *59*, 6059.

[24] S. Yan, X. Liu, W. J. Liu, H. Lan, H. Wu, *Mater. Sci. Eng. A* **2015**, *640*, 137.

[25] M. G. Mecozzi, J. Eiken, M. J. Santofimia, J. Sietsma, *Comp. Mater. Sci.* **2016**, *112*, 245.

[26] M. J. Santofimia, J. G. Speer, A. J. Clarke, L. Zhao, J. Sietsma, *Acta Mater.* **2009**, *57*, 4548.

[27] Y. Takahama, M. J. Santofimia, M. G. Mecozzi, L. Zhao, J. Sietsma, *Acta Mater.* **2012**, *60*, 2916.

[28] N. Luzginova, L. Zhao, J. Sietsma, *Mater. Sci. Eng. A* **2007**, *448*, 104.

[29] M. Amirthalingam, M. J. M. Hermans, L. Zhao, I. M. Richardson, *Metall. Mater. Trans. A* **2010**, *41*, 431.

[30] A. Bojack, L. Zhao, P. F. Morris, J. Sietsma, *Metall. Mater. Trans. A* **2014**, *45*, 5956.

[31] R. Honeycombe, H. K. D. H. Bhadeshia, *Steels, Microstructure and Properties*, 2nd ed., Edward Arnold, London **1981**.

[32] D. P. Koistinen, R. E. Marburger, *Acta Metall.* **1959**, *7*, 59.

[33] S. M. C. van Bohemen, *Scr. Mater.* **2013**, *69*, 315.

[34] S. M. C. van Bohemen, *Mater. Sci. Tech.* **2012**, *28*, 487.

[35] L. Cheng, C. M. Brakman, B. M. Korevaar, E. J. Mittemeijer, *Metall. Trans. A* **1988**, *19*, 2415.

[36] H. Kong, Q. Chao, M. H. Cai, E. J. Pavlina, B. Rolfe, P. D. Hodgson, H. Beladi, *Mater. Sci. Eng. A* **2017**, *707*, 538.

[37] M. J. Santofimia, R. H. Petrov, L. Zhao, J. Sietsma, *Mater. Charact.* **2014**, *92*, 91.

[38] C. F. Jatczak, J. A. Larson, S. W. Shin, *Retained Austenite and Its Measurements by X-Ray Diffraction*, SAE Inc., Warrendale, PA **1980**.

[39] L. Zhao, N. M. van der Pers, J. Sietsma, S. van der Zwaag, *Mater. Sci. Forum* **2005**, *500–501*, 379.

[40] M. Witte, C. Lesch, *Mater. Charact.* **2018**, *139*, 111.

[41] L. Zhao, N. H. van Dijk, E. Brück, J. Sietsma, S. van der Zwaag, *Mater. Sci. Eng. A* **2001**, *313*, 145.

[42] T. T. W. Koopmans, Master Thesis, Delft University of Technology, **2015**.

[43] L. Zhao, N. H. van Dijk, A. J. E. Lefering, J. Sietsma, *J. Mater. Sci.* **2013**, *48*, 1474.

[44] W. Solano-Alvarez, H. F. G. Abreu, M. R. da Silva, M. J. Peet, *J. Magn. Magn. Mater.* **2015**, *378*, 200.

[45] R. T. van Tol, L. Zhao, J. Sietsma, *Acta Mater.* **2014**, *64*, 33.

[46] J. G. Speer, E. De Moor, K. O. Findley, D. K. Matlock, B. C. De Cooman, D. V. Edmonds, *Metall. Mater. Trans. A* **2011**, *42*, 3591.

[47] A. Bojack, L. Zhao, P. F. Morris, J. Sietsma, *Metall. Mater. Trans. A* **2016**, *47*, 1996.